Acclimation of photosynthetic capacity and foliar respiration in Andean tree species to temperature change

Andrew J. F. Cox[1] (iD), Iain P. Hartley[1] (iD), Patrick Meir[2,3] (iD), Stephen Sitch[1] (iD), Mirindi Eric Dusenge[1,4,5] (iD), Zorayda Restrepo[6,7] (iD), Sebastian González-Caro[1,7] (iD), Juan Camilo Villegas[6], Johan Uddling[4] (iD) and Lina M. Mercado[1,7] (iD)

[1]Geography, Faculty of Environment, Science and Economy, University of Exeter, Exeter, EX4 4RKJ, UK; [2]School of Geosciences, University of Edinburgh, Edinburgh, EH9 3JN, UK; [3]Division of Plant Sciences, Research School of Biology, The Australian National University, Canberra, ACT 2601, Australia; [4]Department of Biological and Environmental Sciences, University of Gothenburg, PO Box 461, Gothenburg SE-405 30, Sweden; [5]Department of Biology, The University of Western Ontario, London, ON N6A 3K7, Canada; [6]Grupo de Investigación en Ecología Aplicada, Universidad de Antioquia, Medellín, Colombia; [7]UK Centre for Ecology and Hydrology, Crowmarsh-Gifford, Wallingford, OX10 8BB, UK

Authors for correspondence:
Andrew J. F. Cox
Email: ac644@exeter.ac.uk

Lina M. Mercado
Email: L.Mercado@exeter.ac.uk

Summary

- Climate warming is causing compositional changes in Andean tropical montane forests (TMFs). These shifts are hypothesised to result from differential responses to warming of cold- and warm-affiliated species, with the former experiencing mortality and the latter migrating upslope. The thermal acclimation potential of Andean TMFs remains unknown.
- Along a 2000 m Andean altitudinal gradient, we planted individuals of cold- and warm-affiliated species (under common soil and irrigation), exposing them to the hot and cold extremes of their thermal niches, respectively. We measured the response of net photosynthesis (A_{net}), photosynthetic capacity and leaf dark respiration (R_{dark}) to warming/cooling, 5 months after planting.
- In all species, A_{net} and photosynthetic capacity at 25°C were highest when growing at growth temperatures (T_g) closest to their thermal means, declining with warming and cooling in cold-affiliated and warm-affiliated species, respectively. When expressed at T_g, photosynthetic capacity and R_{dark} remained unchanged in cold-affiliated species, but the latter decreased in warm-affiliated counterparts. R_{dark} at 25°C increased with temperature in all species, but remained unchanged when expressed at T_g.
- Both species groups acclimated to temperature, but only warm-affiliated species decreased R_{dark} to photosynthetic capacity ratio at T_g as temperature increased. This could confer them a competitive advantage under future warming.

Introduction

Tropical montane forests (TMFs) cover *c.* 8% (> 1000 m above sea level (asl)) of tropical forest area and are being increasingly recognised as globally important carbon sinks (Scatena *et al.*, 2010; Spracklen & Righelato, 2014). Aboveground carbon stocks in African TMFs are estimated to be as high as their lowland counterparts (Cuni-Sanchez *et al.*, 2021), and in South America, the Andean TMF carbon sink may be stronger, per unit area, than that of mature lowland forests in Amazonia, Africa and southeast Asia (Duque *et al.*, 2021). Despite Andean forests being significant carbon stores (Duque *et al.*, 2021), biodiversity hotspots (Myers *et al.*, 2000) and essential sources of freshwater and hydroelectricity for millions of people (Josse *et al.*, 2009; Anderson *et al.*, 2011), their responses to future warming remain highly uncertain (Booth *et al.*, 2012; Friedlingstein *et al.*, 2014).

Recent increases in heat extremes have most keenly affected tropical regions (Coumou & Robinson, 2013), and the tropics will be the first part of the globe to experience historically unprecedented levels of warming, with mean temperatures predicted to regularly exceed bounds of historical variability by 2050 (Mora *et al.*, 2013). Warming in the tropics is fastest at high elevation (> 1000 m asl; Ruiz-Carrascal *et al.*, 2012) and is amplified by factors such as changing atmospheric humidity, where even small increases in water vapour can substantially increase the amount of longwave radiation intercepted at the surface (Pepin *et al.*, 2015), leading to further warming. Maximum temperatures in the northern tropical Andes have increased 1.2–6.6°C for the period 1950–2007 (Ruiz-Carrascal *et al.*, 2012), and global climate models suggest maximum daily temperatures could further increase by up to 5°C by 2100 in montane regions (Pabón-Caicedo *et al.*, 2020). The stable thermal conditions during the Holocene (Janzen, 1967; Perez *et al.*, 2016) may have caused TMFs to become adjusted to narrow climate bounds, rendering them particularly sensitive to climate warming (Dusenge *et al.*, 2021). Increased maximum temperatures have negative

effects on tropical wood productivity (Hubau *et al.*, 2020; Sullivan *et al.*, 2020), and recent, rapid warming in the northern Andes has been associated with directional changes in community composition: species from lower elevations ('warm-affiliated') are increasing in abundance across elevations at the expense of those from higher elevations ('cold-affiliated'; Feeley *et al.*, 2011, 2012; Duque *et al.*, 2015; Rehm & Feeley, 2015; Fadrique *et al.*, 2018). This compositional change, termed 'thermophilisation', has been detected on both adult and juvenile trees. Thermophilisation in Andean forests is hypothesised to be caused by increased mortality of cold-affiliated species in the warmer portion of their thermal ranges and the simultaneous upward migration of warm-affiliated species at the cooler ends of their ranges (Duque *et al.*, 2015; Fadrique *et al.*, 2018). There remains, however, a limited understanding of the exact mechanisms behind the observed compositional changes and of the physiological responses of TMFs to future warming (van de Weg *et al.*, 2012; Bahar *et al.*, 2017).

If plants are to adjust their physiology in response to warming, they must undergo short-term, physiological changes to alter their rates of photosynthesis and respiration through a collection of processes, together known as thermal acclimation (Crous, 2019). Successful leaf-level photosynthetic acclimation to a new growth temperature (T_g) results in net photosynthesis (A_{net}), maximum rates of carbon fixation by the enzyme Rubisco (V_{cmax}) and RuBP regeneration by the electron transport chain (J_{max}) being maintained or upregulated (Way & Yamori, 2014; Dusenge *et al.*, 2015; Kumarathunge *et al.*, 2019), while respiratory acclimation leads to leaf-level dark respiration (R_{dark}) being equal or lower at the new temperature (Slot & Kitajima, 2015). Partial acclimation can also occur, where rates of A_{net}, V_{cmax}, J_{max} or R_{dark} are adjusted to a change in temperature, but not sufficiently to be deemed beneficial to the plant (Way & Yamori, 2014; Slot & Kitajima, 2015). Enzymatic reactions are faster at higher temperatures, allowing plants to achieve optimal CO_2 assimilation with lower levels of photosynthetic enzymes (Arcus *et al.*, 2016; Smith & Keenan, 2020; Wang *et al.*, 2020); this should result in warm-acclimated plants exhibiting lower rates of both V_{cmax} and J_{max} than cool-acclimated plants of the same species when measured at a common temperature (Way & Oren, 2010; Ali *et al.*, 2015; Vårhammar *et al.*, 2015; Bahar *et al.*, 2017; Wang *et al.*, 2017, 2020; Dusenge *et al.*, 2021). However, previous work on the responses of these parameters to warming is mixed, with studies reporting decreases (Dusenge *et al.*, 2020, 2021), increases (Crous *et al.*, 2013) and no change (Scafaro *et al.*, 2017; Crous *et al.*, 2018, 2022; Fauset *et al.*, 2019; Choury *et al.*, 2022) in rates of V_{cmax} and J_{max} at 25°C with warming. R_{dark} is tightly coupled with V_{cmax} (Atkin *et al.*, 2015; Wang *et al.*, 2020) due to a large proportion of respiratory energy being required to synthesise and maintain photosynthetic proteins (O'Leary *et al.*, 2019), including the highly abundant Rubisco (Raven, 2013; Bar-On & Milo, 2019). Conversely, studies across biomes consistently report thermal acclimation of R_{dark}, with lower rates expressed at a common temperature in warm-grown plants compared with cool-grown plants (Reich *et al.*, 2016; Slot & Winter, 2017; Smith

et al., 2019; Mujawamariya *et al.*, 2021), but as respiration and photosynthesis are usually studied separately it is uncertain to what extent these reductions are linked to photosynthetic capacity and overall plant carbon budgets.

Although temperature is a key determinant of A_{net}, V_{cmax}, J_{max} and R_{dark} rates, water and nutrient availability also have an important influence over these processes. If temperatures rise without a concomitant increase in water availability, higher vapour pressure deficit (VPD) will lower stomatal conductance (g_s), reducing carbon fixation, transpiration and causing leaf temperatures to rise (Lin *et al.*, 2015). In the sunlit leaves of some TMF species, the combination of stomatal closure and high irradiance can cause leaf temperatures to exceed air temperatures by up to 18°C, possibly surpassing optimum temperatures (T_{opt}) of key physiological processes (Fauset *et al.*, 2018; Tarvainen *et al.*, 2022). Without effective thermal acclimation, this could cause substantial reductions in photosynthetic rates in Andean TMFs (Miller *et al.*, 2021). The macronutrients nitrogen (N) and phosphorus (P) are also heavily invested in photosynthesis and respiration (Evans, 1989; Domingues *et al.*, 2015); indeed, several studies have reported a strong correlation between photosynthetic capacity and R_{dark} with leaf N and P (Atkin *et al.*, 2015; Domingues *et al.*, 2015; Rowland *et al.*, 2017; Mujawamariya *et al.*, 2021; Ellsworth *et al.*, 2022). The foliar concentrations of these nutrients have been found to vary with elevation – for example, Mujawamariya *et al.* (2021) report highest area-based N (N_a) at high elevation along an elevation gradient in Rwanda – and between species in TMFs (Ziegler *et al.*, 2020), but further work is needed to determine the extent to which they may influence V_{cmax}, J_{max} and R_{dark} in Andean ecosystems (but see van de Weg *et al.*, 2012; Bahar *et al.*, 2017). Warming can also significantly increase soil mineralisation rates in as little as 2 yr (Rustad *et al.*, 2001), so it is also important to consider potential indirect temperature effects on foliar nutrients and therefore photosynthetic capacity and respiration.

Evolutionary history may be a key determinant of how different species respond to warming. Species that originate from warmer lowland forests and that persisted during historical warm periods (Zachos *et al.*, 2008; Dick *et al.*, 2013) are more likely to possess higher T_{opt} for physiological processes, due to conservative evolution of upper thermal limits through time (Lancaster & Humphreys, 2020; Bennett *et al.*, 2021), than those historically found in, and adapted to, the cooler highlands. Due to the slow evolution of thermal tolerance, there is limited scope for adaptation to heat resistance with rapid warming (Araújo *et al.*, 2013; Bennett *et al.*, 2021), and cold-affiliated Andean species may be close to the upper thermal limits of their metabolism (O'Sullivan *et al.*, 2017; Feeley *et al.*, 2020) when growing at the hot extremes of their thermal distributions. Indeed, many native Andean TMF species are most abundant when growing at temperatures close to the mean of their thermal ranges, suggesting greater fitness under these conditions (Arellano & Macía, 2014; Arellano *et al.*, 2014); therefore, cold-affiliated Andean TMF species may be at a competitive disadvantage under continued warming.

Plants in boreal and temperate ecosystems acclimate V_{cmax} and J_{max} to large seasonal temperature changes by shifting their

photosynthetic T_{opt} upward in response to warming, while R_{dark} is acclimated by downregulating respiratory rates (Campbell *et al.*, 2007; Sendall *et al.*, 2015). Thermal acclimation has also been observed in lowland tropical forest species (Cheesman & Winter, 2013; Carter *et al.*, 2020), though the observed extent of thermal acclimation potential in the tropics is reported to be lower than in mid- and high-latitude species (Slot & Winter, 2017). Thus far, the thermal acclimation potential of TMFs to warming has been understudied compared with other ecosystems, with the most extensive work coming from an elevation gradient in Rwanda. This has found variable responses to warming in Afromontane forests: Dusenge *et al.* (2021) reported that two montane species acclimated to a *c.* 7°C temperature rise by reducing rates of V_{cmax} and J_{max}, with others observing that cold-adapted species may be particularly sensitive to warming (Vårhammar *et al.*, 2015; Tito *et al.*, 2020; Wittemann *et al.*, 2022). Strong thermal acclimation of R_{dark} to *c.* 5°C of warming, regardless of species, has also been observed (Mujawamariya *et al.*, 2021). A major shortcoming of previous acclimation studies, however, is that many are conducted using potted seedlings (Dusenge *et al.*, 2021), or using potted seedlings in highly controlled growing environments (Cheesman & Winter, 2013; Slot & Winter, 2017; Crous *et al.*, 2018; Choury *et al.*, 2022; Wittemann *et al.*, 2022), so little is known about the responses of freely rooted trees growing under field conditions (but see Mujawamariya *et al.* (2021) for R_{dark}). Understanding the thermal acclimation potential of a variety of Andean TMF species is key to comprehending current observed compositional changes in these ecosystems and to predict how ecosystem composition might be altered by further warming.

Here, we use the natural warming of a tropical elevation gradient to examine the thermal acclimation potential of A_{net}, V_{cmax}, J_{max} and R_{dark} to rising temperatures (Nooten & Hughes, 2017; Tito *et al.*, 2020). We focus on eight mid-successional species of both cold- and warm-affiliated origin, dominant in TMFs in the Colombian Andes. We use three common garden plantations along a 2000 m elevation/temperature gradient (14°C, 22°C and 26°C) in the northwest Colombian Andes, where we have exposed cold- and warm-affiliated species to temperatures close to their geographical thermal means but also to the hot and cold extremes of their thermal niches, respectively. Our investigation was guided by the following hypotheses:

H1: A_{net}, V_{cmax} and J_{max} will be highest when species are growing at temperatures closest to their thermal means ('home') and will decrease with displacement from their home temperature.

H2: Warm-affiliated species will demonstrate greater fitness when transplanted to temperatures below their home temperatures than cold-affiliated species transplanted to temperatures above their home temperatures, with fitness evaluated in terms of A_{net}, R_{dark} : V_{cmax} and greater investment in photosynthetic capacity (V_{cmax}, J_{max}). This will provide support for the observed thermophilisation in Andean TMFs.

H3: The direct effect of warming or cooling on V_{cmax}, J_{max} and R_{dark} of cold- and warm-affiliated species, respectively, will dominate over potential indirect temperature effects of soil warming and changing mineralisation rates.

Materials and Methods

Common garden experiment and plant material

We transplanted 15 dominant Colombian TMF species across three sites along a 2000 m elevation gradient in the northwest Colombian Andes. These sites (Table 1) are geographically close to one another but with differing mean annual temperatures (MAT), precipitation (MAP), and minimum and maximum temperatures. Seeds of all tree species were collected from the forest neighbouring the 14°C experimental site and propagated in poly-pots for 24 months in a nursery located at a site with MAT of 22°C. Planting height varied between 50 and 100 cm (depending on species). Saplings were then transplanted to the three experimental sites from November to December 2018, with each planted in the ground. These were planted in common soils (400 kg per tree) sourced from a high-elevation site with similar characteristics to a forest adjacent to the 14°C site. Each site was arranged as four plots (the experimental unit), each consisting of six blocks, with one individual from each species planted in each block (15 species × 6 blocks × 4 plots = 360 plants per site; Supporting Information Fig. S1). The sixth block of each plot was fertilised every 4 months ('fertilised') to give similar but artificially high soil nutrient content, while the remaining five blocks were untreated ('non-fertilised'); this gave four fertilised trees per species, per site, from which any indirect effects of soil warming on nutrient availability and plant productivity could be determined.

The experiment includes 11 cold- and 4 warm-affiliated species with different thermal distributions. For this study, we selected species with leaves that fit the chamber of the LI-6800 portable photosynthesis system (Li-Cor Inc., Lincoln, NE, USA): two warm-affiliated species from the *Inga* genus which are abundant at low elevations, and six cold-affiliated species common to high elevations (Fig. 1; Table S1). Measurements of all species

Table 1 Key characteristics of the study sites.

	High elevation (14°C)	Mid-elevation (22°C)	Low elevation (26°C)
Location (latitude, longitude)	5.54°N, −75.68°W	5.60°N, −75.62°W	6.01°N, −75.85°W
Elevation (m asl)	2516	1357	736
MAT (°C)	14.1	21.8	25.9
T_{day} (°C)	16.1	22.5	27.1
T_{night} (°C)	12.6	19.6	22.7
T_{min} (1 ‰; °C)	9.7	16.8	20.4
T_{max} (99 ‰; °C)	33.1	39.2	44.2
(mm yr^{-1})	2774	2045	2298
Mean VPD (kPa)	0.82	1.14	1.83
VPD (99 ‰; kPa)	2.284	3.478	4.439

The high-elevation site has a mean annual temperature (MAT) of *c.* 14°C ('14°C site'), mid-elevation of *c.* 22°C ('22°C site') and low elevation of *c.* 26°C ('26°C site'). Daytime temperature (T_{day}) was calculated from mean temperatures 06:00–18:00, while night-time temperature (T_{night}) is mean temperatures 18:00–06:00. T_{min} is minimum temperature, T_{max} is maximum temperature, and MAP is mean annual precipitation. Mean vapour pressure deficit (VPD) was calculated using daytime (06:00–18:00) VPD values.
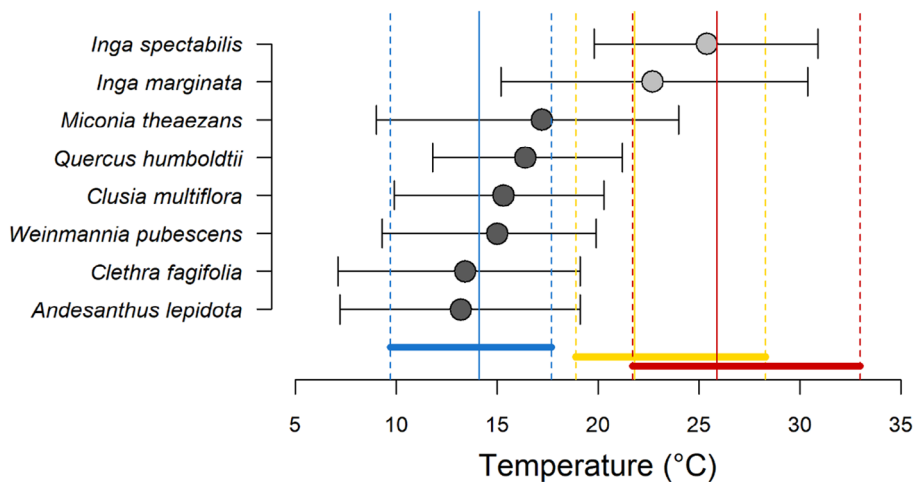
Fig. 1 Tree species in this study and their thermal distributions: thermal means (grey dots for warm-affiliated and black dots for cold-affiliated), maxima and minima (vertical lines at the end of each horizontal line) were extracted from worldclim (Fick & Hijmans, 2017) for all locations where study species have been recorded. Biological records were taken from the Global Biodiversity Information Facility. For each site, dashed vertical lines show the diurnal temperature range, and solid vertical lines the thermal mean: blue for the 14°C site, yellow for the 22°C site and red for the 26°C site.

were taken at the 14°C (nonfertilised = 32, fertilised = 26) and 22°C (nonfertilised = 30, fertilised = 18) sites, but were limited to the two warm-affiliated species at 26°C (nonfertilised = 8, fertilised = 8) due to mortality of all cold-affiliated species at this site.

Gas exchange measurements

Leaf gas exchange measurements were conducted *in situ* between June and August 2019 from fully expanded and visibly healthy sunlit leaves on the top branches of individuals using a LI-6800 portable photosynthesis system. All photosynthesis measurements were collected between 09:00 and 15:00, and only after leaf g_s had stabilised at ≥ 0.05 mol m^{-2} s^{-1} to conditions inside the LI-6800 cuvette. Upon clamping onto a leaf, conditions inside the cuvette were standardised to 29°C, 65% relative humidity and 410 ppm CO_2; once stable, net photosynthesis was measured sequentially at eight different ambient CO_2 concentrations (C_a; 410, 300, 175, 60, 410, 800, 1500 and 2000) corresponding to different intercellular C_i concentrations to produce CO_2 response (A–C_i) curves, with light intensity being set to a predetermined saturating photon flux density (PPFD) for each species (Table S2). A common leaf temperature of 29°C, within the diurnal range at all sites (see T_{min} and T_{max} in Table 1; Fig. S2), was selected as a compromise to give comparable raw A–C_i data across sites. VPD and g_s during A–C_i measurements are shown in Fig. S3. R_{dark} data were collected from the same leaves as A–C_i measurements; these were covered with aluminium foil straight after A–C_i measurements, for at least 30 min (sometimes for several hours) to become dark-adapted (Scafaro *et al.*, 2017), after which CO_2 efflux from leaves was measured using the LI-6800 at 5-s intervals for 1 min between 15:00 and 16:00. This gave 12 values, the mean of which was taken to be R_{dark}. All R_{dark} measurements were taken at the ambient temperature of each site.

Leaf structure and nutrient analysis

Following gas exchange measurements, leaves were immediately collected for determination of leaf mass per unit area (M_a) and

foliar N and P for standardisation of photosynthetic capacity and leaf respiration parameters on mass and nutrient bases. First, leaves were sealed in individually labelled plastic bags containing damp cotton wool and placed out of direct sunlight in order to prevent premature drying. Every evening, images of each leaf were taken with a CanoScan LiDE 300 flatbed scanner. Area values for each leaf were then returned by using the LeafArea package in the R environment (Katabuchi, 2015; v.4.2.1, R Core Team, 2022), which automates the ImageJ program (Schneider *et al.*, 2012). Leaves were weighed before being dried in an oven for 48 h at 70°C. They were then reweighed to give their dry mass, allowing M_a values to be calculated.

To determine leaf nutrient concentrations, dried leaf samples were ground into a fine powder using a shaker mill (model MM400; Retsch, Hann, Germany) and *c.* 1 mg of sample for each leaf was packed into tin capsules and run through an isotope ratio mass spectrometer (model Integra2 Integrated EA-IRMS; Sercon Ltd, Crewe, UK) to return leaf C and N concentrations. For leaf P concentrations, 0.1–0.2 g of sample was subjected to ICP-OES analysis with a unique Dichroic Spectral Combiner (model 5110; Agilent Technologies, Santa Clara, CA, USA).

Derivation of V_{cmax}, J_{max} and R_{dark} and sensitivity to their parameterisation

The A–C_i curves were fitted with Farquhar *et al.* (1980)'s model of C$_3$ photosynthesis, carried out in R using the curve-fitting procedure from the PLANTECOPHYS package (Duursma, 2015) to derive rates of V_{cmax} and J_{max} (Methods S1). Measured R_{dark} values were included in the curve-fitting procedure, accounting for 30% light inhibition of respiration during the day (Atkin *et al.*, 2000; Tcherkez *et al.*, 2012, 2017). R_{dark} values were also adjusted to the A–C_i measurement temperature using Eqn 1 to account for the temperature sensitivity of respiration (Eqn 1; Tjoelker *et al.*, 2001; Heskel *et al.*, 2016):

$$R = R_{Tref} \times Q_{10}^{\frac{T - T_{ref}}{10}} \qquad \text{Eqn 1}$$

where R is the rate of respiration measured with the LI-6800 at measurement temperature T (°C), Q_{10} is the proportional change in respiration per 10°C increase in temperature (Atkin & Tjoelker, 2003), R_{Tref} is the rate of respiration at the chosen reference temperature, and, in this case, T_{ref} is the A–C_i measurement temperature (°C). We included the temperature dependence of Q_{10} (Eqn 2; Tjoelker *et al.*, 2001):

$$Q_{10} = 3.09 - 0.043\,T_g \qquad \text{Eqn 2}$$

where T_g is the MAT at our study sites (14°C, 22°C or 26°C). Eqns 1, 2, were also used to estimate R_{dark} at 25°C ($R_{\mathrm{dark\_25}}$) and site growth temperature ($R_{\mathrm{dark\_Tg}}$) to assess respiratory acclimation potential. R_{dark} values were compared against values estimated with a constant Q_{10} of 2 (often used in modelling studies; Clark *et al.*, 2011) and a Q_{10} of 2.3, which has been used in various previous tropical forest studies (Meir *et al.*, 2001; Atkin & Tjoelker, 2003; Weerasinghe *et al.*, 2014; Slot & Winter, 2017; Mujawamariya *et al.*, 2021).

As part of the A–C_i fitting procedure in 'plantecophys', differences in atmospheric pressure with altitude were also included (Eqn S1), as this influences substrate availability for Rubisco (Wang *et al.*, 2017, 2020). After fitting the A–C_i curves, the estimates of V_{cmax} and J_{max} were quality-checked; 144 of 147 estimates were retained, and of these, a further nine J_{max} values were excluded after quality control. V_{cmax} and J_{max} values were returned on a leaf area basis, and these were then adjusted to both a reference temperature of 25°C ($V_{\mathrm{cmax\_25}}$; $J_{\mathrm{max\_25}}$) and to the respective air temperatures at each site ($V_{\mathrm{cmax\_Tg}}$; $J_{\mathrm{max\_Tg}}$) using Eqn 3:

$$f(T_k) = k_{25}\exp\left[\frac{E_a(T_k - 298)}{298 R T_k}\right]\frac{1 + \exp\left(\frac{298\Delta S - H_d}{298 R}\right)}{1 + \exp\left(\frac{T_k \Delta S - H_d}{T_k R}\right)} \qquad \text{Eqn 3}$$

where E_a is the activation energy of V_{cmax} or J_{max} (J mol^{-1}), T_k is leaf temperature (°K), R is the universal gas constant (8.314 J mol^{-1} K^{-1}), ΔS is the entropy value for V_{cmax} or J_{max} (J mol^{-1} K^{-1}), and H_d is a deactivation value for V_{cmax} or J_{max}.

We tested the sensitivity of V_{cmax} and J_{max} values to the temperature response parameterisation (Eqn 3), using parameters from an Afromontane forest species, *Carapa grandiflora* (Vårhammar *et al.*, 2015) and those of Kumarathunge *et al.* (2019; see their Table 2) that are derived from a global dataset and account for thermal acclimation via a dependence on T_{growth} of E_{aV}, ΔS_v and ΔS_J in Eqn 3. V_{cmax} and J_{max} estimated using the Kumarathunge *et al.* (2019) parameters and the three sets of R_{dark} Q_{10} values (2, 2.3 and temperature dependent) were also compared against one another. One-way ANOVAs and Tukey *post hoc* tests were used to test the differences among parameterisations using the LM package in R.

Data analysis

All analyses were performed in R. To assess the ability of different species to thermally acclimate photosynthetic capacity and foliar

dark respiration, we compared V_{cmax}, J_{max}, R_{dark}, $J_{\mathrm{max}} : V_{\mathrm{cmax}}$ and $R_{\mathrm{dark}} : V_{\mathrm{cmax}}$ at 25°C and T_g on area, mass, N and P bases across growth temperatures, as well as A_{net} measured at 29°C. Owing to the differing thermal affiliations (Fig. 2) and temperature responses of cold- and warm-affiliated species, our results present these groups separately. Two-way ANOVA and Tukey *post hoc* tests were used to test for significant differences in values between both temperature treatments and between cold- and warm-affiliated groups ('species groups') at each site (Table 2). These were complemented by mixed-effects ANOVA tests with the NLME package (Pinheiro *et al.*, 2021), with temperature treatment and species groups set as main effects, and species nested within species groups as a random effect (Table S3). Additionally, one-way ANOVA tests were used to test for differences between cold-affiliated and *Inga spectabilis* at 22°C, as at this site the groups were at the upper and lower limits of their thermal ranges, respectively (Table S4). Residuals were visually checked for normality before ANOVA tests were undertaken. Nonfertilised plants were analysed to test H1 and H2, while values for nonfertilised and fertilised plants were compared to address H3. One-way ANOVAs were used to test for significant differences between nonfertilised and fertilised plants. As an additional test for whether species could acclimate to new growing temperatures, we produced scatterplots to compare values of A_{net}, $V_{\mathrm{cmax\_25}}$, $J_{\mathrm{max\_25}}$ and $R_{\mathrm{dark\_25}}$ at 'home' and 'away' temperatures for each species (Fig. S4; Table S5).

Results

Sensitivity analysis to temperature response parameters

When calculating V_{cmax}, J_{max} and R_{dark} at 25°C and T_{growth} using three different Q_{10} values (2, 2.3 and temperature-dependent Q_{10}), at each site, there were no significant differences between the mean values of V_{cmax}, J_{max} and R_{dark} (Table S6). After comparing V_{cmax} and J_{max} values at 25°C using two sets of temperature response parameters for montane species – *C. grandiflora* from Vårhammar *et al.* (2015), and those including thermal acclimation of temperature optima of V_{cmax} and J_{max} (Kumarathunge *et al.*, 2019), there were no significant differences between the mean values of V_{cmax} and J_{max} at each site (Table S7). Any conclusions derived from our results were consequently unaffected by the temperature response parameters used.

Impacts of warming on photosynthesis and photosynthetic capacity

A_{net} at 29°C, $V_{\mathrm{cmax\_25}}$ and $J_{\mathrm{max\_25}}$ were highest in cold- and warm-affiliated species at 14°C and 26°C, respectively (Fig. 2), which are the sites with growth temperatures closest to their species' thermal means (Fig. S4). Species-level results are given in Figs S7–S9. Growth temperature had pronounced effects on $V_{\mathrm{cmax\_25}}$ and $V_{\mathrm{cmax\_Tg}}$ across sites. In cold-affiliated species ($n = 6$), $V_{\mathrm{cmax\_25}}$ decreased by 39% (3.83 µmol m^{-2} s^{-1} per degree of warming) between 14°C and 22°C (Fig. 2; Table 3), as well as on mass and N bases (Fig. S5). $V_{\mathrm{cmax\_Tg}}$ remained constant
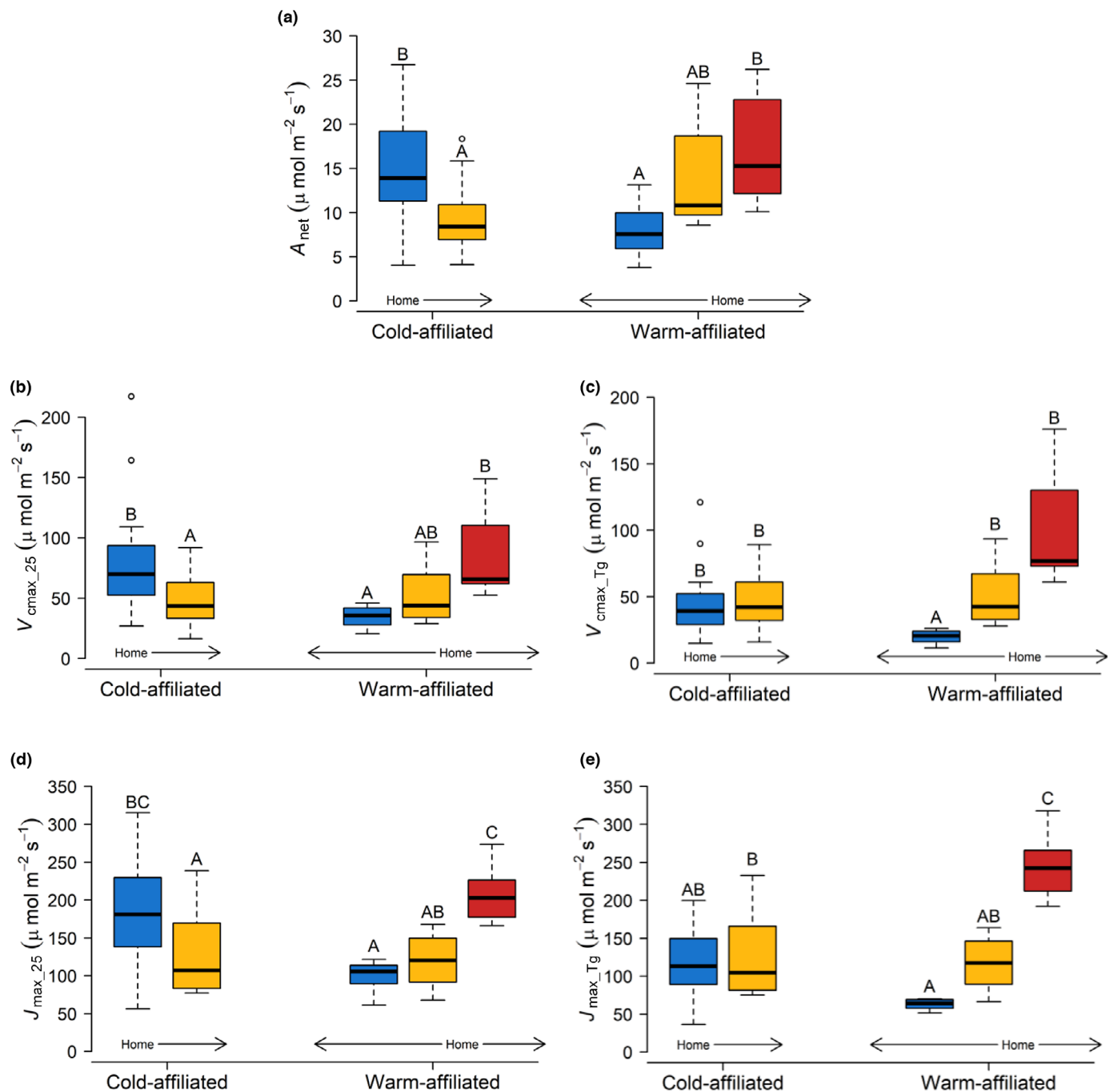
Fig. 2 Impacts of temperature change on rates of net photosynthesis (A_{net}) measured at 29°C (a), as well as photosynthetic capacity (V_{cmax} and J_{max}) on a leaf area basis (µmol m^{-2} s^{-1}) at both 25°C (b, d) and growth temperature (T_g; c, e). Species are grouped into cold- ($n = 6$) and warm-affiliated ($n = 2$), and colours represent the different temperature treatments (14°C, blue; 22°C, yellow; 26°C, red). 'Home' shows the home temperature for each species group (14°C for cold-affiliated; 22–26°C for warm-affiliated), and arrows indicate if they were subjected to warming or cooling. Upper and lower edges of each box indicate the 75th and 25th percentiles, respectively, while the horizontal line is the median and vertical bars indicate the 90th and 10th percentile ranges. Open circles above/below boxes denote outliers. Capital letters are used for comparisons between boxes, where a difference denotes a significant difference, at least at the $P < 0.05$ level from Tukey *post hoc* tests (apart from panel (b), where the difference between 'cold-affiliated' 22°C and 'warm-affiliated' 26°C is $P < 0.06$). Full results are given in Table 2.

(Fig. 2), although it was significantly higher at 22°C on a N basis (Fig. S6). For warm-affiliated species ($n = 2$), the same effect was observed with cooling, particularly for *I. spectabilis*, where V_{cmax_25} decreased by 67% (5.99 µmol m^{-2} s^{-1} per degree of cooling) between 26°C and 14°C. For both warm-affiliated

species, V_{cmax_Tg} decreased by 80% between 26°C and 14°C (Fig. 2), with decreases also seen on mass, N and P bases (Figs S5, S6).

Similar changes were seen in J_{max_25} and J_{max_Tg} with changing temperature. In cold-affiliated species, area-based J_{max_25} was

Table 2 Outputs of two-way ANOVAs and Tukey *post hoc* tests for the effect of site (i.e. temperature) on maximum rate of carboxylation by Rubisco (V_{cmax}), maximum rate of electron transport (J_{max}), leaf dark respiration (R_{dark}), ratio of J_{max} to V_{cmax} ($J_{max} : V_{cmax}$) and ratio of R_{dark} to V_{cmax} ($R_{dark} : V_{cmax}$) at 25°C and growth temperature (T_g), as well as net photosynthesis (A_{net}) measured at 29°C, for cold- ('C') and warm-affiliated ('W') species.

	V_{cmax_25}	J_{max_25}	R_{dark_25}	$J_{max\_25} : V_{cmax\_25}$	$R_{dark\_25} : V_{cmax\_25}$	A_{net}
25°C						
(df$_{site}$, df$_{residual}$)	(4, 65)	(4, 64)	(4, 64)	(4, 63)	(4, 65)	(4, 65)
C14°C–C22°C	**0.02**	**0.03**	**0.02**	0.86	0.96	**0.01**
W14°C–W22°C	0.85	0.98	**0.03**	0.44	**< 0.001**	0.15
W14°C–W26°C	**0.03**	**0.004**	**0.02**	0.88	**< 0.001**	**0.008**
W22°C–W26°C	0.42	**0.04**	1.00	0.97	0.49	0.91
C14°C–W14°C	**0.02**	**0.009**	0.25	0.35	**< 0.001**	**0.03**
C14°C–W22°C	0.51	0.12	0.52	0.99	0.99	1.00
C14°C–W26°C	0.99	0.85	0.41	0.99	0.53	0.77
C22°C–W14°C	0.92	0.83	**< 0.001**	0.86	**< 0.001**	0.98
C22°C–W22°C	1.00	1.00	0.95	0.88	1.00	0.21
C22°C–W26°C	**0.06***	**0.01**	0.90	0.99	0.22	**0.005**

	V_{cmax_Tg}	J_{max_Tg}	R_{dark_Tg}	$J_{max\_Tg} : V_{cmax\_Tg}$	$R_{dark\_Tg} : V_{cmax\_Tg}$
T_{growth}					
(df$_{site}$, df$_{residual}$)	(4, 65)	(4, 61)	(4, 61)	(4, 59)	(4, 65)
C14°C–C22°C	0.99	0.99	0.23	1.00	0.82
W14°C–W22°C	0.12	0.21	0.34	0.34	**< 0.001**
W14°C–W26°C	**< 0.001**	**< 0.001**	0.09	0.79	**< 0.001**
W22°C–W26°C	**0.004**	**< 0.001**	0.99	0.96	0.11
C14°C–W14°C	**< 0.001**	0.07	0.64	0.87	**< 0.001**
C14°C–W22°C	0.99	1.00	**0.003**	0.73	0.61
C14°C–W26°C	0.53	**< 0.001**	**< 0.001**	1.00	0.59
C22°C–W14°C	**< 0.001**	**0.03**	1.00	0.71	**< 0.001**
C22°C–W22°C	1.00	0.99	0.20	0.89	0.97
C22°C–W26°C	0.22	**< 0.001**	**0.02**	1.00	0.15

For example, 'C14°C–C22°C' compares cold-affiliated values at the 14°C and 22°C sites. The '*' for 'C22°C–W26°C' indicates an almost significant result at the $P < 0.05$ level. Bold text indicates any significant value at the $P < 0.05$ level or below.
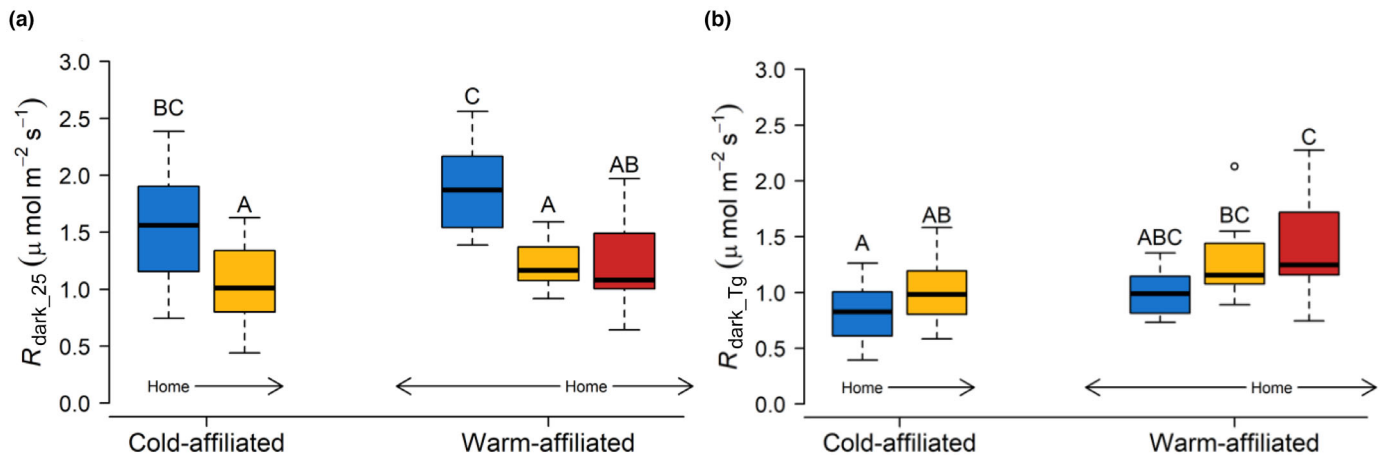

Fig. 3 Impacts of temperature change on rates of R_{dark} on a leaf area basis (µ mol m^{-2} s^{-1}) at both 25°C (a) and growth temperature (T_g; b). Species are grouped into cold- ($n = 6$) and warm-affiliated ($n = 2$), and colours represent the different temperature treatments (14°C, blue; 22°C, yellow; 26°C, red). 'Home' shows the home temperature for each species group (14°C for cold-affiliated; 22–26°C for warm-affiliated), and arrows indicate if they were subjected to warming or cooling. Upper and lower edges of each box indicate the 75th and 25th percentiles, respectively, while the horizontal line is the median and vertical bars indicate the 90th and 10th percentile ranges. Open circles above/below boxes denote outliers. Capital letters are used for comparisons between boxes, where a difference denotes a significant difference, at least at the $P < 0.05$ level from Tukey *post hoc* tests. Full results are given in Table 2.

29% lower (6.52 µmol m^{-2} s^{-1} per degree of warming) at the 22°C than the 14°C site, while J_{max_Tg} was unchanged. In warm-affiliated species, the response to cooling was nonlinear, with large declines between 26°C and 22°C of 21.68 and 31.71 µmol m^{-2} s^{-1} per degree of cooling for J_{max_25} and J_{max_Tg}, respectively, largely driven by *I. spectabilis* (Fig. 2; Table 3). Decreases

in J_{max_25} and J_{max_Tg} for warm-affiliated species with cooling were also observed when expressed on mass, N and P bases, while few changes were observed in cold-affiliated species (Figs S5, S6). The ratio of J_{max} to V_{cmax} ($J_{max} : V_{cmax}$) remained unchanged in both cold- and warm-affiliated species at 25°C and T_g (Fig. 4a,b; Table 2). At the species level, only one species responded significantly to warming in the cold-affiliated group (Figs S7, S8).

Impacts of changing growth temperature on dark respiration

R_{dark_25} decreased with increasing temperature in all species. In cold-affiliated species, R_{dark_25} declined by 31% between 14°C and 22°C, and in warm-affiliated species, R_{dark_25} increased with cooling from 26°C and 14°C by 27% for *I. spectabilis*, and by 37% for *I. marginata* between 22°C and 14°C (Fig. 3; Table 3). At T_g, the pattern was very different, with R_{dark_Tg} remaining constant with temperature change across sites for both cold- and warm-affiliated species (Fig. 3; Table 2), deviating greatly from the significant decreases with cooling observed for V_{cmax_Tg} (Fig. 2; Table 2). On mass, N and P bases, $R_{dark,25}$ either decreased or remained constant for cold-affiliated species, while warm-affiliated remained constant or increased with cooling (Fig. S5), but R_{dark_Tg} in warm-affiliated species decreased with cooling (expressed in N, P and mass basis) and increased with warming in their cold-affiliated counterparts (expressed in N and P basis; Fig. S6). Corresponding species-level responses are shown in Fig. S10. Cold-affiliated species kept their ratio of R_{dark}

to V_{cmax} ($R_{dark} : V_{cmax}$) constant with warming, and warm-affiliated species displayed increases of 292% and 284% with cooling between 26°C and 14°C when expressed at 25°C and T_g, respectively (Fig. 4).

Impact of fertilisation

There was no evidence to suggest that changes in rates of V_{cmax}, J_{max} and R_{dark} on area basis at 25°C and T_g were influenced by soil warming (Fig. S11; Table S8). For cold- and warm-affiliated species, there were no significant differences between rates in nonfertilised and fertilised plants in any instance, indicating that direct temperature effects dominate over any potential indirect temperature effects in our dataset.

Discussion

We have investigated the physiological responses to temperature change in Andean TMF trees that are freely rooted in common, irrigated soils and growing under field conditions. Our results show that all species, except *I. marginata*, have highest A_{net}, V_{cmax_25} and J_{max_25} when growing closest to their home environment, with values decreasing at temperatures away from their thermal means. When values were expressed at T_g, V_{cmax} and J_{max} were homeostatic with warming in cold-affiliated species, while these metrics decreased with cooling in warm-affiliated species, possibly suggesting greater plasticity of photosynthetic capacity in cold- than warm-affiliated species. R_{dark_25} declined with warming in cold-

Table 3 Acclimation potential of maximum rate of carboxylation by Rubisco (V_{cmax}), maximum rate of electron transport (J_{max_25}) and leaf dark respiration (R_{dark}) in tropical species, normalised to 25°C.

Study	Type of dataset	V_{cmax_25} (µmol m^{-2} s^{-1} °C^{-1})	J_{max_25} (µmol m^{-2} s^{-1} °C^{-1})	R_{dark_25} (µmol m^{-2} s^{-1} °C^{-1})
This study:	Field-grown, juvenile trees	3.83	6.52	0.06
Cold-affiliated (14–22°C)		5.99	11.43	0.05
Inga spectabilis (26–14°C)		0.61	0.07	0.08
Inga marginata (22–14°C)				
Choury *et al*. (2022):	Glasshouses, potted seedlings	4.20	9.53	–
[2]*Atractocarpus fitzalanii* (27.5–34.5°C)		2.16	6.91	–
[2]*Xanthostemon chrysanthus* (27.5°C–34.5°C)				
Crous *et al*. (2018):	Glasshouses, potted juvenile trees	0.47	1.08	–
[2]*Eucalyptus tereticornis* (28.5–32°C)		1.97	0.11	–
[2]*Eucalyptus grandis* (28.5–32°C)				
Dusenge *et al*. (2021):	Field-grown, potted seedlings	5.69	14.43	
[1]*Harungana montana* (15.1–20°C)		2.44	6.52	
[1]*Syzygium guineense* (15.1–20°C)				
[1]Mujawamariya *et al*. (2021) (15.2–20.6°C)	Field-grown, juvenile trees	–	–	0.11*
[2]Scafaro *et al*. (2017) (15–25°C)	Glasshouses, potted seedlings	0.73	1.58	–
[1]Wittemann *et al*. (2022) (20–30°C)	Glasshouses, potted seedlings	0.73	1.40	0.04

This is expressed as the change per degree of warming or cooling (°C) for cold- and warm-affiliated species (*Inga spectabilis* and *Inga marginata*) in our study, respectively, compared with changes in montane and lowland forest species derived from other studies. The growth temperatures used for each study/species/species group are given in brackets in the first column. Acclimation potentials of [1]montane and [2]lowland tropical rainforest species from other studies are given. The Mujawamariya *et al*. (2021) R_{dark} value is the average of 10 early-successional and six late-successional species, standardised to 20°C rather than 25°C*. The Scafaro *et al*. (2017) and Wittemann *et al*. (2022) values are averages of four species.
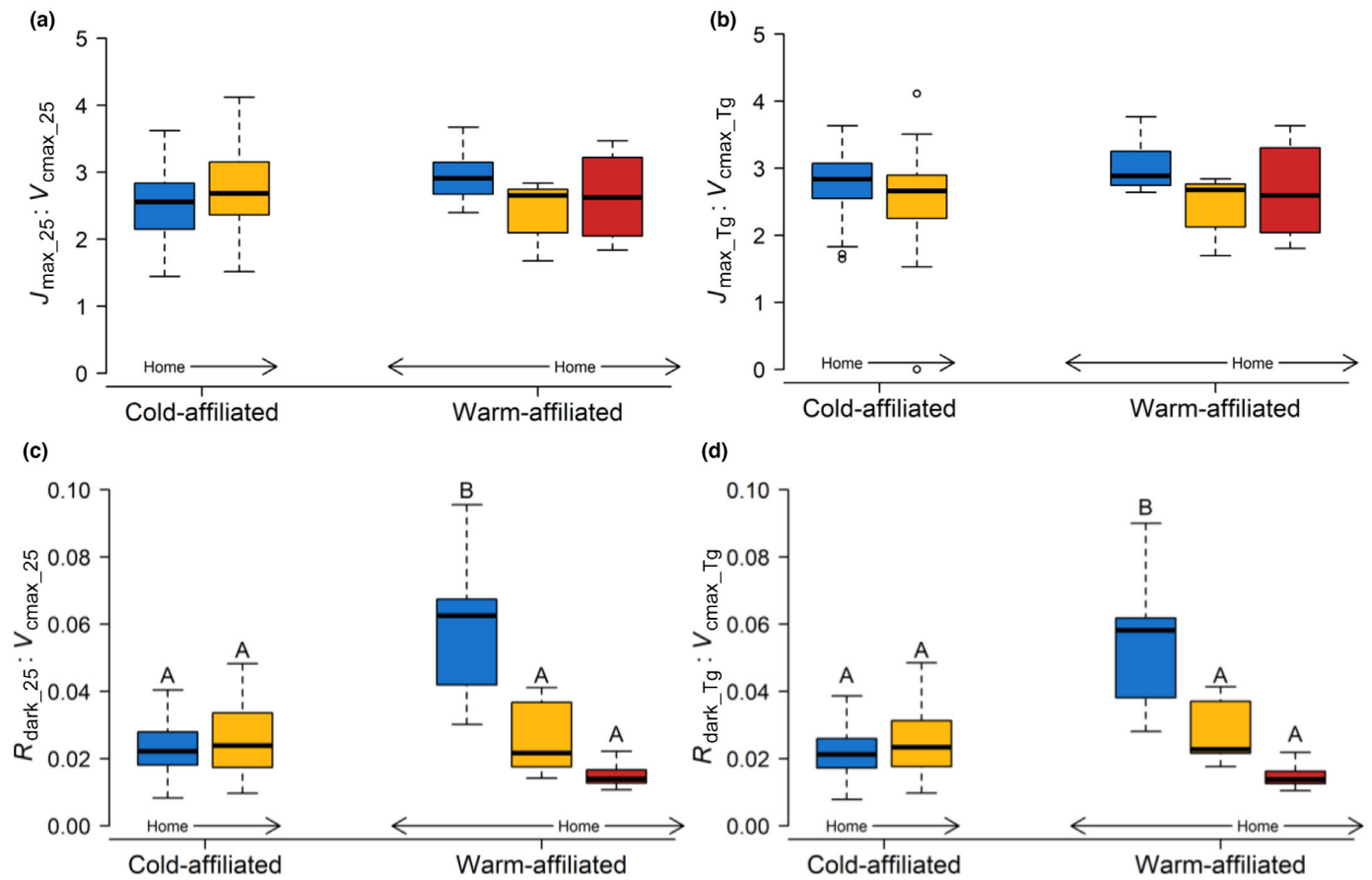
Fig. 4 Ratios of $J_{max} : V_{cmax}$ and $R_{dark} : V_{cmax}$ at 25°C (a, c) and site growth temperature (b, d) on leaf area basis (μ mol m^{-2} s^{-1}). Species are grouped into cold- ($n = 6$) and warm-affiliated ($n = 2$), and colours represent the different temperature treatments (14°C, blue; 22°C, yellow; 26°C, red). 'Home' shows the home temperature for each species group (14°C for cold-affiliated; 22–26°C for warm-affiliated), and arrows indicate if they were subjected to warming or cooling. Upper and lower edges of each box indicate the 75th and 25th percentiles, respectively, while the horizontal line is the median and vertical bars indicate the 90th and 10th percentile ranges. Open circles above/below boxes denote outliers. Capital letters are used for comparisons between boxes, where a difference denotes a significant difference, at least at the $P < 0.05$ level from Tukey *post hoc* tests. Full results are given in Table 2.

affiliated species and increased with cooling in warm-affiliated species; at T_g, R_{dark} remained constant in both cold- and warm-affiliated species, suggesting that complete acclimation occurred. Cold-affiliated species failed to improve carbon-use efficiency (by not lowering their $R_{dark} : V_{cmax}$) with warming, while warm-affiliated species significantly increased this with cooling, suggesting that they are less efficient at colder temperatures.

Photosynthetic capacity and respiration in TMFs

The V_{cmax_25}, J_{max_25} and R_{dark_25} in our cold-affiliated species at 14°C are of the same order of magnitude as previously reported for high-elevation TMF species (Table 4). The V_{cmax_25} and J_{max_25} values are similar to those of early-successional TMF species in Rwanda (Ziegler *et al.*, 2020; Dusenge *et al.*, 2021), while in Peru, they are at the upper end of values reported by van de Weg *et al.* (2012) but are much higher than those of Bahar *et al.* (2017). The R_{dark_25} values from both Peru (van de Weg *et al.*, 2012) and Rwanda (Ziegler *et al.*, 2020; Mujawamariya *et al.*, 2021) are comparable to our cold-affiliated values at 14°C.

Photosynthetic capacity and leaf dark respiration in the warm-affiliated species at 26°C are at the high end of those reported by similar studies (Table 3). These disparities could not be explained by the higher photosynthetic capacities of younger trees (Kitajima *et al.*, 2002), as Dusenge *et al.* (2021) and Mujawamariya *et al.* (2021) conducted their measurements on seedlings and juveniles, respectively. The acquisitive life strategies, naturally fast growth rates and association with N-fixing bacteria of many *Inga* species (Franche *et al.*, 2009; dos Santos Pereira *et al.*, 2019) may therefore be more accountable for the observed differences.

Thermal acclimation in Andean TMFs

In this study, V_{cmax_25} and J_{max_25} decreased in cold-affiliated species when transplanted away from their home elevation and exposed to warm extremes, but were higher at these temperatures in their warm-affiliated counterparts, with a similar pattern being found for A_{net} (Fig. 2; Table 2). The responses of cold-affiliated species to higher temperatures are in agreement with previously reported observations (Way & Oren, 2010; Ali *et al.*, 2015; Scafaro *et al.*, 2017; Dusenge *et al.*, 2021) and

Table 4 Maximum rate of carboxylation by Rubisco (V_{cmax}), maximum rate of electron transport (J_{max}) and leaf dark respiration (R_{dark}) values, standardised to 25°C, for our cold- and warm-affiliated species at home elevation, as well as for 26°C for *Inga marginata*, compared with those of other studies of tropical and tropical montane species.

Study	Dataset – type and location	V_{cmax_25} (µmol m^{-2} s^{-1})	J_{max_25} (µmol m^{-2} s^{-1})	R_{dark_25} (µmol m^{-2} s^{-1})
This study:	Field-grown, juvenile trees;	77.59 ± 8.73	180.07 ± 14.26	1.53 ± 0.09
Cold-affiliated at 14°C	Colombian Andes	108.12 ± 18.08	235.17 ± 13.86	1.51 ± 0.19
Inga spectabilis at 26°C		38.03 ± 4.77 (61.35 ± 3.22)	102.66 ± 15.86 (177.94 ± 5.53)	1.08 ± 0.06 (0.93 ± 0.10)
Inga marginata at 22°C (26°C)				
Bahar *et al.* (2017):	Field-grown, mature trees;	35.9 ± 14.6	66.7 ± 18.6	–
[1]Upland species	Colombian Andes	48.8 ± 20.0	96.9 ± 36.9	–
[2]Lowland species				
Dusenge *et al.* (2021):	Field-grown, potted	62.17 ± 2.98	148.95 ± 6.74	–
[1]*Harungana montana* (early-successional)	seedlings; Albertine Rift, Rwanda	53.22 ± 2.00	127.11 ± 8.46	–
[1]*Syzygium guineense* (late-successional)				
[1]Mujawamariya *et al.* (2021)	Field-grown, juvenile trees; Albertine Rift, Rwanda	–	–	1.88 ± 0.05*
[1]van de Weg *et al.* (2012)	Field-grown, mature trees; Peruvian Andes	40–80	65–160	1.4–2
Ziegler *et al.* (2020):	Field-grown, mature trees;	71 ± 9.0	171 ± 21.0	1.6 ± 0.1
[1]Early-successional TMF	Albertine Rift, Rwanda	45 ± 3.0	102 ± 6.0	1.2 ± 0.1
[1]Late-successional TMF				

Standard error values are given where available. Values for cold-affiliated species are those from the 14°C site, while warm-affiliated are from the 26°C and 22°C sites. For the other studies, there is a mix of montane[1] and lowland forest[2] species, with data collected from trees growing at their home elevations. Values from van de Weg *et al.* (2012) are a range of top-canopy measurements from five species. For Bahar *et al.* (2017), 'Upland species' is the mean value from these species at their upland sites (MAT 8.0–18.8°C) and 'Lowland species' the mean value from these species at their lowland sites (MAT 24.4–26.2°C). Values from Dusenge *et al.* (2021) are means from their high-elevation site (MAT 15.1°C).
*Here, the R_{dark} value from Mujawamariya *et al.* (2021) has been standardised to 25°C rather than the 20°C reported in the study.

could be partially explained by optimality theory (Arcus *et al.*, 2016; Smith & Keenan, 2020; Wang *et al.*, 2020). The reductions caused by warming in N-based V_{cmax_25} (Fig. S5), as well as the lower mass-based N (N_m) of cold-affiliated species found in a larger dataset from this elevation gradient (1.54 ± 0.06 g g^{-1} at 14°C and 1.34 ± 0.06 g g^{-1} at 22°C, $P < 0.05$), could indicate lower concentrations of photosynthetic enzymes in warm-grown plants, particularly Rubisco, which requires large amounts of N investment (Bahar *et al.*, 2017; Dusenge *et al.*, 2021). Indeed, Bahar *et al.* (2017) conducted laboratory assays into leaf protein content on an elevation gradient in the Peruvian Andes and reported significantly lower Rubisco concentrations – as well as area and N-based V_{cmax_25}, and N_a – in warm-grown leaves compared with cool-grown leaves collected from the field. Conversely, the warm-affiliated species, which were exposed to the cold extremes of their thermal distributions, exhibit higher V_{cmax_25} and J_{max_25} at higher growth temperatures (i.e. photosynthetic capacity declines with cooling) which are closer to their home environment, while foliar N_m remained constant. This could be explained by their higher thermal means (Fig. 1), suggesting that these species might have higher T_{opt} for V_{cmax} and J_{max} at 22°C (*I. marginata*) and 26°C (*I. spectabilis*). Consequently, the A_{net}, V_{cmax_25} and J_{max_25} responses to growth temperature agree with our H1.

Although R_{dark_25} decreased with warming in cold-affiliated species and increased with cooling in warm-affiliated counterparts, patterns changed when values were expressed at growth temperature: both cold- and warm-affiliated species showed no

change, even with an 8°C temperature change for the former and 12°C for the latter (Fig. 3). The lack of change in R_{dark_Tg} indicates that both species groups are able to completely acclimate respiration rates (R_{dark_Tg} remains constant) to substantial changes in temperature, which was also was found by Mujawamariya *et al.* (2021), although they additionally observe some overcompensatory (R_{dark_Tg} decreased with temperature change) acclimation in Rwandan TMF species. However, species in their study were exposed to only 5°C of warming (Mujawamariya *et al.*, 2021), so whether overcompensatory acclimation would be found with further warming of +8°C or greater is unclear.

Thermal acclimation of photosynthetic capacity is rarely reported at T_g in thermal acclimation studies in the tropics (but see Malhi *et al.*, 2017); here, we find that cold-affiliated species maintain V_{cmax_Tg} and J_{max_Tg} between 14°C and 22°C, while warm-affiliated species greatly decrease photosynthetic capacity from 22°C to 14°C, as well as from 26°C to 22°C (Fig. 2). There are, however, no significant differences in V_{cmax} or J_{max} values (at 25°C or T_g) between cold-affiliated species and *I. spectabilis* at 22°C (H2), the site where both groups have been transplanted away from their home environment (Table S4). As V_{cmax} controls the substrate available for respiration (Wang *et al.*, 2017, 2020; O'Leary *et al.*, 2019) and respiratory energy is needed to maintain the turnover of proteins involved in photosynthetic metabolism (Rowland *et al.*, 2017), these two parameters are often coordinated in their temperature response (Dusenge *et al.*, 2021). However, in warm-affiliated species there is no change in R_{dark_Tg} with temperature, while photosynthetic capacity is significantly

higher at 26°C. This results in an increase in $R_{dark\_Tg} : V_{cmax\_Tg}$ with cooling (Fig. 3d) reducing carbon-use efficiency (Rowland *et al.*, 2017). However, under climate warming, warm-affiliated species will benefit from increased carbon-use efficiency. Given that at 22°C, both species groups have the same R_{dark_Tg}: V_{cmax_Tg} and A_{net}, this indicates similar physiological fitness at this growth temperature (partially rejecting H2), thus permitting warm-affiliated species to compete with cold-affiliated plants and helping to explain the thermophilisation being observed in Andean TMFs (partially supporting H2; Duque *et al.*, 2015; Fadrique *et al.*, 2018).

Patterns in R_{dark_Tg} (Fig. 3) generally follow those observed for both V_{cmax_Tg} and J_{max_Tg} (Fig. 2), with V_{cmax_Tg} explaining 50% of the observed variation in R_{dark_Tg} in both cold- and warm-affiliated species (Fig. S12). Indeed, V_{cmax} controls the substrate available for respiration (Wang *et al.*, 2017, 2020; O'Leary *et al.*, 2019) and respiratory energy is needed to maintain the turnover of proteins involved in photosynthetic metabolism (Rowland *et al.*, 2017), and similar findings have recently been reported by Dusenge *et al.* (2021) for two Rwandan TMF species. In warm-affiliated species, there is no change in R_{dark_Tg} with temperature, while photosynthetic capacity is significantly higher at 26°C. This results in a large reduction in R_{dark_Tg}: V_{cmax_Tg} with warming (Fig. 3d), indicating a greater carbon-use efficiency (Rowland *et al.*, 2017) that may allow warm-affiliated species to grow much faster than cold-affiliated species under warmer conditions.

Interspecific variability in temperature responses

Evidence suggests that the catalytic efficiency of Rubisco may differ in species that have evolved under contrasting thermal regimes (Andersson & Backlund, 2008; Kumarathunge *et al.*, 2019) so that with current climatic warming Rubisco kinetic properties may be improved in some species more than others to grant greater affinity for CO_2 and increased rates of carbon fixation (Galmés *et al.*, 2014). Our warm-affiliated species are from *Inga*, a large neotropical genus that diversified from the warmer climes of Amazonia in the past 2–10 million yr, with phylogenetic analysis revealing that *Inga* persisted during this time period in far warmer temperatures than are currently experienced in Amazonia (Richardson *et al.*, 2001; Zachos *et al.*, 2008; Dick *et al.*, 2013). The genus is now distributed across South America in a variety of habitats (Richardson *et al.*, 2001; Endara & Jaramillo, 2011; Palow *et al.*, 2012; Nicholls *et al.*, 2015; dos Santos Pereira *et al.*, 2019), so considerable thermal plasticity may exist in *Inga* species. The two *Inga* species in our study exhibit their highest V_{cmax_25} at 26°C (home environment), indicating that their Rubisco may be optimised to warmer conditions, but they were able to downregulate this by 7.73 and 4.17 μmol m^{-2} s^{-1} °C^{-1} with 4°C and 12°C of cooling, respectively (Fig. 2a; Table 3), suggesting an ability to acclimate to colder conditions. Although this acclimation does not improve the fitness of warm-affiliated species (Way & Yamori, 2014), it enables them to persist at temperatures beyond the cold extremes of their thermal range. Conversely, the cold-affiliated species downregulated their V_{cmax_25}

by 3.83 μmol m^{-2} s^{-1} per degree of warming between 14°C and 22°C (Fig. 2a; Table 3), demonstrating a large thermal acclimation potential. This agrees with findings from the late-successional Rwandan TMF species, *S. guineense* (Dusenge *et al.*, 2021; Table 3), but differs from temperate species (Kattge & Knorr, 2007) and a global, seasonal dataset of tropical, temperate and boreal species (Kumarathunge *et al.*, 2019), which finds no changes in V_{cmax_25} or J_{max_25} with variation in growth temperature but a decrease in $J_{max\_25} : V_{cmax\_25}$ with warming, whereas our results (Fig. 4a) and those of Dusenge *et al.* (2021) and other tropical studies (Scafaro *et al.*, 2017; Crous *et al.*, 2018) find no change in $J_{max\_25} : V_{cmax\_25}$ with increased growth temperature. A constant $J_{max\_25} : V_{cmax\_25}$ suggests that carboxylation has not become limited by warming (in cold-affiliated species) or cooling (in warm-affiliated species) inducing lower g_s or higher photorespiration (Dusenge *et al.*, 2021). Overall, the observed responses to temperature-induced changes in V_{cmax_25} and J_{max_25} in this and other TMF studies (e.g. Dusenge *et al.*, 2021) suggest that TMF species may possess a greater ability to acclimate to warming than has been previously hypothesised for species in tropical latitudes (Janzen, 1967; Cunningham & Read, 2003).

Life strategies may also elicit differences in photosynthetic and respiratory rates, and their responses to warming, between TMF species. Although our study focusses on mid-successional species, *Inga* species are typically classed as pioneers, performing well in high light conditions and frequently involved in the early stages of forest restoration and regeneration (dos Santos Pereira *et al.*, 2019). Indeed, early-successional species exhibit higher rates of photosynthesis than late-successional species in elevation gradient studies in Rwanda (Vårhammar *et al.*, 2015; Dusenge *et al.*, 2021). *Inga* species also have a symbiotic relationship with N-fixing bacteria (Franche *et al.*, 2009); the high light environments of our study sites, coupled with the significantly greater foliar N concentrations in *Inga* species compared with the others in our study (N$_a$ = $P < 0.05$; N$_m$ = $P < 0.001$; P$_m$ = $P < 0.05$), could explain differences in V_{cmax}, J_{max} and R_{dark} between species groups (Figs 2, 3).

Direct vs indirect temperature effects

Soil nutrient content did not significantly affect photosynthetic or respiratory rates, supporting H3; thus, changes in air temperature are the dominant influence (Rustad *et al.*, 2001; Classen *et al.*, 2015; Fig. S10; Table S8). Transplanting common soils to be used across sites ensured that all plants were growing in a similar medium at the outset of the experiment, but the warmer temperatures of 22°C and 26°C could have affected soil microbial communities, changing decomposition and nutrient mineralisation rates to alter the availability of key macro- and micronutrients (Rustad *et al.*, 2001; Classen *et al.*, 2015). Although we find some significant differences in foliar P content between sites – for example, between 14°C and 22°C for cold-affiliated species in P$_m$ – the absence of any significant differences in rates of V_{cmax}, J_{max} or R_{dark} between nonfertilised and fertilised plants (Fig. S10; Table S8) strongly suggests that variability between sites is driven

by temperature. Although other environmental variables do vary along elevation gradients, including insolation and wind speed (Körner, 2007; Sundqvist *et al.*, 2013; Tito *et al.*, 2020), transplant experiments are still far more effective than glasshouse or growth chamber experiments (Cheesman & Winter, 2013; Slot & Winter, 2017; Fauset *et al.*, 2019; Wittemann *et al.*, 2022) for assessing the impact of changing temperatures at the ecosystem level and over long time periods (Nooten & Hughes, 2017; Tito *et al.*, 2020).

The physiological adaptation and acclimation of warm- and cold-affiliated species to different temperatures could have implications for the composition of Andean TMFs with continued warming this century. Our study demonstrates that dominant species are able to acclimate to considerable warming and cooling through adjustments to photosynthetic capacity and R_{dark}, with all species exhibiting their highest V_{cmax}, J_{max} and A_{net} at temperatures close to their thermal distribution means. As warm-affiliated species can acclimate to cooler temperatures and also excel at high temperatures, we could expect to see shifts in Andean TMFs towards these species as temperatures rise.

Acknowledgements

Competing interests

None declared.

Author contributions

The research was designed by LMM, with contributions from AJFC, IPH and PM. LMM, IPH, PM, JCV, JU and SS wrote the grants that have funded the research. ZR, LMM and JCV established the study sites where AJFC and LMM conducted field measurements. AJFC analysed the data and wrote the manuscript, with important contributions from LMM, IPH, PM, SS, MED, JU, JCV and SG-C.

ORCID

Andrew J. F. Cox https://orcid.org/0000-0002-5166-7169
Mirindi Eric Dusenge https://orcid.org/0000-0003-4218-0911
Sebastian González-Caro https://orcid.org/0000-0002-2287-7431
Iain P. Hartley https://orcid.org/0000-0002-9183-6617
Patrick Meir https://orcid.org/0000-0002-2362-0398
Lina M. Mercado https://orcid.org/0000-0003-4069-0838
Zorayda Restrepo https://orcid.org/0000-0002-3213-9985
Stephen Sitch https://orcid.org/0000-0003-1821-8561
Johan Uddling https://orcid.org/0000-0003-4893-1915

Data availability

The data that support the findings of this study are publicly available from the UK CEH Environmental Information Data Centre: https://doi.org/10.5285/60dd0b8f-f0c3-4e30-841b-1c2067052974.

References

Ali AA, Xu C, Rogers A, McDowell NG, Medlyn BE, Fisher RA, Wullschleger SD, Reich PB, Vrugt JA, Bauerle WL et al. 2015. Global-scale environmental control of plant photosynthetic capacity. *Ecological Applications* 25: 2349–2365.

Anderson EP, Marengo J, Villalba R, Halloy S, Young B, Cordero D, Gast F, Jaimes E, Ruiz D, Herzog SK. 2011. Consequences of climate change for ecosystems and ecosystem services in the tropical Andes. In: Herzog SK, Martinez R, Jørgensen PM, Tiessen H, eds. *Climate change and biodiversity in the tropical Andes.* Inter-American Institute for Global Change Research (IAI) and Scientific Committee on Problems of the Environment (SCOPE), 1–18.

Andersson I, Backlund A. 2008. Structure and function of Rubisco. *Plant Physiology and Biochemistry* 46: 275–291.

Araújo MB, Ferri-Yáñez F, Bozinovic F, Marquet PA, Valladares F, Chown SL. 2013. Heat freezes niche evolution. *Ecology Letters* 16: 1206–1219.

Arcus VL, Prentice EJ, Hobbs JK, Mulholland AJ, Van der Kamp MW, Pudney CR, Parker EJ, Schipper LA. 2016. On the temperature dependence of enzyme-catalyzed rates. *Biochemistry* 55: 1681–1688.

Arellano G, Cala V, Macía MJ. 2014. Niche breadth of oligarchic species in Amazonian and Andean rain forests. *Journal of Vegetation Science* 25: 1355–1366.

Arellano G, Macía MJ. 2014. Local and regional dominance of woody plants along an elevational gradient in a tropical montane forest of northwestern Bolivia. *Plant Ecology* 215: 39–54.

Atkin OK, Bloomfield KJ, Reich PB, Tjoelker MG, Asner GP, Bonal D, Bönisch G, Bradford MG, Cernusak LA, Cosio EG et al. 2015. Global variability in leaf respiration in relation to climate, plant functional types and leaf traits. *New Phytologist* 206: 614–636.

Atkin OK, Evans JR, Ball MC, Lambers H, Pons TL. 2000. Leaf respiration of snow gum in the light and dark. Interactions between temperature and irradiance. *Plant Physiology* 122: 915–924.

Atkin OK, Tjoelker MG. 2003. Thermal acclimation and the dynamic response of plant respiration to temperature. *Trends in Plant Science* 8: 343–351.

Bahar NH, Ishida FY, Weerasinghe LK, Guerrieri R, O'Sullivan OS, Bloomfield KJ, Asner GP, Martin RE, Lloyd J, Malhi Y et al. 2017. Leaf-level photosynthetic capacity in lowland Amazonian and high-elevation Andean tropical moist forests of Peru. *New Phytologist* 214: 1002–1018.

Bar-On YM, Milo R. 2019. The global mass and average rate of rubisco. *Proceedings of the National Academy of Sciences, USA* 116: 4738–4743.

Bennett JM, Sunday J, Calosi P, Villalobos F, Martínez B, Molina-Venegas R, Araújo MB, Algar AC, Clusella-Trullas S, Hawkins BA et al. 2021. The evolution of critical thermal limits of life on Earth. *Nature Communications* 12: 1198.

Booth BB, Jones CD, Collins M, Totterdell IJ, Cox PM, Sitch S, Huntingford C, Betts RA, Harris GR, Lloyd J. 2012. High sensitivity of future global warming to land carbon cycle processes. *Environmental Research Letters* 7: 024002.

Campbell C, Atkinson L, Zaragoza-Castells J, Lundmark M, Atkin O, Hurry V. 2007. Acclimation of photosynthesis and respiration is asynchronous in response to changes in temperature regardless of plant functional group. *New Phytologist* 176: 375–389.

Carter KR, Wood TE, Reed SC, Schwartz EC, Reinsel MB, Yang X, Cavaleri MA. 2020. Photosynthetic and respiratory acclimation of understory shrubs in response to *in situ* experimental warming of a wet tropical forest. *Frontiers in Forests and Global Change* 3: 765–785.

Cheesman AW, Winter K. 2013. Growth response and acclimation of CO_2 exchange characteristics to elevated temperatures in tropical tree seedlings. *Journal of Experimental Botany* 64: 3817–3828.

Choury Z, Wujeska-Klause A, Bourne A, Bown NP, Tjoelker MG, Medlyn BE, Crous KY. 2022. Tropical rainforest species have larger increases in temperature optima with warming than warm-temperate rainforest trees. *New Phytologist* 234: 1220–1236.

Clark DB, Mercado LM, Sitch S, Jones CD, Gedney N, Best MJ, Pryor M, Rooney GG, Essery RLH, Blyth E *et al.* 2011. The Joint UK Land Environment Simulator (JULES), model description–Part 2: carbon fluxes and vegetation. *Geoscientific Model Development* 4: 701–722.

Classen AT, Sundqvist MK, Henning JA, Newman GS, Moore JA, Cregger MA, Moorhead LC, Patterson CM. 2015. Direct and indirect effects of climate change on soil microbial and soil microbial–plant interactions: what lies ahead? *Ecosphere* 6: 1–21.

Coumou D, Robinson A. 2013. Historic and future increase in the global land area affected by monthly heat extremes. *Environmental Research Letters* 8: 034018.

Crous KY. 2019. Plant responses to climate warming: physiological adjustments and implications for plant functioning in a future, warmer world. *American Journal of Botany* 106: 1049–1051.

Crous KY, Drake JE, Aspinwall MJ, Sharwood RE, Tjoelker MG, Ghannoum O. 2018. Photosynthetic capacity and leaf nitrogen decline along a controlled climate gradient in provenances of two widely distributed *Eucalyptus* species. *Global Change Biology* 24: 4626–4644.

Crous KY, Quentin AG, Lin YS, Medlyn BE, Williams DG, Barton CV, Ellsworth DS. 2013. Photosynthesis of temperate *Eucalyptus globulus* trees outside their native range has limited adjustment to elevated CO_2 and climate warming. *Global Change Biology* 19: 3790–3807.

Crous KY, Uddling J, De Kauwe MG. 2022. Temperature responses of photosynthesis and respiration in evergreen trees from boreal to tropical latitudes. *New Phytologist* 234: 353–374.

Cuni-Sanchez A, Sullivan MJ, Platts PJ, Lewis SL, Marchant R, Imani G, Hubau W, Abiem I, Adhikari H, Albrecht T *et al.* 2021. High aboveground carbon stock of African tropical montane forests. *Nature* 596: 536–542.

Cunningham SC, Read JJNP. 2003. Do temperate rainforest trees have a greater ability to acclimate to changing temperatures than tropical rainforest trees? *New Phytologist* 157: 55–64.

Dick CW, Lewis SL, Maslin M, Bermingham E. 2013. Neogene origins and implied warmth tolerance of Amazon tree species. *Ecology and Evolution* 3: 162–169.

Domingues T, Ishida FY, Feldpausch TR, Grace J, Meir P, Saiz G, Sene O, Schrodt F, Sonké B, Taedoumg H *et al.* 2015. Biome-specific effects of nitrogen and phosphorus on the photosynthetic characteristics of trees at a forest-savanna boundary in Cameroon. *Oecologia* 178: 659–672.

Duque A, Peña MA, Cuesta F, González-Caro S, Kennedy P, Phillips OL, Calderón-Loor M, Blundo C, Carilla J, Cayola L *et al.* 2021. Mature Andean forests as globally important carbon sinks and future carbon refuges. *Nature Communications* 12: 2138.

Duque A, Stevenson PR, Feeley KJ. 2015. Thermophilization of adult and juvenile tree communities in the northern tropical Andes. *Proceedings of the National Academy of Sciences, USA* 112: 10744–10749.

Dusenge ME, Madhavji S, Way DA. 2020. Contrasting acclimation responses to elevated CO_2 and warming between an evergreen and a deciduous boreal conifer. *Global Change Biology* 26: 3639–3657.

Dusenge ME, Wallin G, Gårdesten J, Niyonzima F, Adolfsson L, Nsabimana D, Uddling J. 2015. Photosynthetic capacity of tropical montane tree species in relation to leaf nutrients, successional strategy and growth temperature. *Oecologia* 177: 1183–1194.

Dusenge ME, Wittemann M, Mujawamariya M, Ntawuhiganayo EB, Zibera E, Ntirugulirwa B, Way DA, Nsabimana D, Uddling J, Wallin G. 2021. Limited thermal acclimation of photosynthesis in tropical montane tree species. *Global Change Biology* 27: 4860–4878.

Duursma RA. 2015. Plantecophys - an R package for analysing and modelling leaf gas exchange data. *PLoS ONE* 10: e0143346.

Ellsworth DS, Crous KY, De Kauwe MG, Verryckt LT, Goll D, Zaehle S, Bloomfield KJ, Ciais P, Cernusak LA, Domingues TF *et al.* 2022. Convergence in phosphorus constraints to photosynthesis in forests around the world. *Nature Communications* 13: 5005.

Endara MJ, Jaramillo JL. 2011. The influence of microtopography and soil properties on the distribution of the speciose genus of trees, *Inga* (Fabaceae: Mimosoidea), in Ecuadorian Amazonia. *Biotropica* 43: 157–164.

Evans JR. 1989. Photosynthesis and nitrogen relationships in leaves of C3 plants. *Oecologia* 78: 9–19.

Fadrique B, Báez S, Duque Á, Malizia A, Blundo C, Carilla J, Osinaga-Acosta O, Malizia L, Silman M, Farfán-Ríos W *et al.* 2018. Widespread but heterogeneous responses of Andean forests to climate change. *Nature* 564: 207–212.

Farquhar GD, von Caemmerer SV, Berry JA. 1980. A biochemical model of photosynthetic CO_2 assimilation in leaves of C_3 species. *Planta* 149: 78–90.

Fauset S, Freitas HC, Galbraith DR, Sullivan MJ, Aidar MP, Joly CA, Phillips OL, Vieira SA, Gloor MU. 2018. Differences in leaf thermoregulation and water use strategies between three co-occurring Atlantic forest tree species. *Plant, Cell & Environment* 41: 1618–1631.

Fauset S, Oliveira L, Buckeridge MS, Foyer CH, Galbraith D, Tiwari R, Gloor M. 2019. Contrasting responses of stomatal conductance and photosynthetic capacity to warming and elevated CO_2 in the tropical tree species *Alchornea glandulosa* under heatwave conditions. *Environmental and Experimental Botany* 158: 28–39.

Feeley K, Martinez-Villa J, Perez T, Silva Duque A, Triviño Gonzalez D, Duque A. 2020. The thermal tolerances, distributions, and performances of tropical montane tree species. *Frontiers in Forests and Global Change* 3: 25.

Feeley KJ, Rehm EM, Machovina B. 2012. Perspective: the responses of tropical forest species to global climate change: acclimate, adapt, migrate, or go extinct? *Frontiers of Biogeography* 4: 69–82.

Feeley KJ, Silman MR, Bush MB, Farfan W, Cabrera KG, Malhi Y, Meir P, Revilla NS, Quisiyupanqui MNR, Saatchi S. 2011. Upslope migration of Andean trees. *Journal of Biogeography* 38: 783–791.

Fick SE, Hijmans RJ. 2017. Worldclim 2: New 1-km spatial resolution climate surfaces for global land areas. *International Journal of Climatology.* 37: 4302–4315.

Franche C, Lindström K, Elmerich C. 2009. Nitrogen-fixing bacteria associated with leguminous and non-leguminous plants. *Plant and Soil* 321: 35–59.

Friedlingstein P, Meinshausen M, Arora VK, Jones CD, Anav A, Liddicoat SK, Knutti R. 2014. Uncertainties in CMIP5 climate projections due to carbon cycle feedbacks. *Journal of Climate* 27: 511–526.

Galmés J, Conesa MÀ, Díaz-Espejo A, Mir A, Perdomo JA, Niinemets Ü, Flexas J. 2014. Rubisco catalytic properties optimized for present and future climatic conditions. *Plant Science* 226: 61–70.

Heskel MA, O'sullivan OS, Reich PB, Tjoelker MG, Weerasinghe LK, Penillard A, Egerton JJ, Creek D, Bloomfield KJ, Xiang J *et al.* 2016. Convergence in the temperature response of leaf respiration across biomes and plant functional types. *Proceedings of the National Academy of Sciences, USA* 113: 3832–3837.

Hubau W, Lewis SL, Phillips OL, Affum-Baffoe K, Beeckman H, Cuní-Sanchez A, Daniels AK, CEN E, Fauset S, Mukinzi JM *et al.* 2020. Asynchronous carbon sink saturation in African and Amazonian tropical forests. *Nature* 579: 80–87.

Janzen DH. 1967. Why mountain passes are higher in the tropics. *The American Naturalist* 101: 233–249.

Josse C, Cuesta F, Navarro G, Barrena V, Cabrera E, Chacón-Moreno E, Ferreira W, Peralvo M, Saito J, Tovar A. 2009. *Ecosistemas de los Andes del Norte y Centro.* Bolivia, Colombia, Ecuador, Perú y Venezuela. Lima, Peru: Secretaría General de la Comunidad Andina, Programa Regional ECOBONA-Intercooperation, CONDESAN-Proyecto Páramo Andino,

Programa BioAndes, EcoCiencia, NatureServe, IAvH, LTA-UNALM, ICAE-ULA, CDC-UNALM, RUMBOL SRL.

Katabuchi M. 2015. LEAFAREA: an R package for rapid digital image analysis of leaf area. *Ecological Research* 30: 1073–1077.

Kitajima K, Mulkey SS, Samaniego M, Joseph Wright S. 2002. Decline of photosynthetic capacity with leaf age and position in two tropical pioneer tree species. *American Journal of Botany* 89: 1925–1932.

Kattge J, Knorr W. 2007. Temperature acclimation in a biochemical model of photosynthesis: a reanalysis of data from 36 species. *Plant, Cell & Environment* 30: 1176–1190.

Körner C. 2007. The use of 'altitude' in ecological research. *Trends in Ecology & Evolution* 22: 569–574.

Kumarathunge DP, Medlyn BE, Drake JE, Tjoelker MG, Aspinwall MJ, Battaglia M, Cano FJ, Carter KR, Cavaleri MA, Cernusak LA *et al.* 2019. Acclimation and adaptation components of the temperature dependence of plant photosynthesis at the global scale. *New Phytologist* 222: 768–784.

Lancaster LT, Humphreys AM. 2020. Global variation in the thermal tolerances of plants. *Proceedings of the National Academy of Sciences, USA* 117: 13580–13587.

Lin YS, Medlyn BE, Duursma RA, Prentice IC, Wang H, Baig S, Eamus D, de Dios VR, Mitchell P, Ellsworth DS *et al.* 2015. Optimal stomatal behaviour around the world. *Nature Climate Change* 5: 459–464.

Malhi Y, Girardin CA, Goldsmith GR, Doughty CE, Salinas N. 2017. The variation of productivity and its allocation along a tropical elevation gradient: a whole carbon budget perspective. *New Phytologist* 214: 1019–1032.

Meir P, Grace J, Miranda AC. 2001. Leaf respiration in two tropical rainforests: constraints on physiology by phosphorus, nitrogen and temperature. *Functional Ecology* 15: 378–387.

Miller BD, Carter KR, Reed SC, Wood TE, Cavaleri MA. 2021. Only sun-lit leaves of the uppermost canopy exceed both air temperature and photosynthetic thermal optima in a wet tropical forest. *Agricultural and Forest Meteorology* 301: 108347.

Mora C, Frazier AG, Longman RJ, Dacks RS, Walton MM, Tong EJ, Sanchez JJ, Kaiser LR, Stender YO, Anderson JM *et al.* 2013. The projected timing of climate departure from recent variability. *Nature* 502: 183–187.

Mujawamariya M, Wittemann M, Manishimwe A, Ntirugulirwa B, Zibera E, Nsabimana D, Wallin G, Uddling J, Dusenge ME. 2021. Complete or overcompensatory thermal acclimation of leaf dark respiration in African tropical trees. *New Phytologist* 229: 2548–2561.

Myers N, Mittermeier RA, Mittermeier CG, Da Fonseca GA, Kent J. 2000. Biodiversity hotspots for conservation priorities. *Nature* 403: 853–858.

Nicholls JA, Pennington RT, Koenen EJ, Hughes CE, Hearn J, Bunnefeld L, Dexter KG, Stone GN, Kidner CA. 2015. Using targeted enrichment of nuclear genes to increase phylogenetic resolution in the neotropical rain forest genus *Inga* (Leguminosae: Mimosoideae). *Frontiers in Plant Science* 6: 710.

Nooten SS, Hughes L. 2017. The power of the transplant: direct assessment of climate change impacts. *Climatic Change* 144: 237–255.

O'Leary BM, Asao S, Millar AH, Atkin OK. 2019. Core principles which explain variation in respiration across biological scales. *New Phytologist* 222: 670–686.

O'Sullivan OS, Heskel MA, Reich PB, Tjoelker MG, Weerasinghe LK, Penillard A, Zhu L, Egerton JJ, Bloomfield KJ, Creek D *et al.* 2017. Thermal limits of leaf metabolism across biomes. *Global Change Biology* 23: 209–223.

Pabón-Caicedo JD, Arias PA, Carril AF, Espinoza JC, Borrel LF, Goubanova K, Lavado-Casimiro W, Masiokas M, Solman S, Villalba R. 2020. Observed and projected hydroclimate changes in the Andes. *Frontiers in Earth Science* 8: 61.

Palow DT, Nolting K, Kitajima K. 2012. Functional trait divergence of juveniles and adults of nine *Inga* species with contrasting soil preference in a tropical rain forest. *Functional Ecology* 26: 1144–1152.

Pepin N, Bradley RS, Diaz HF, Baraër M, Caceres EB, Forsythe N, Fowler H, Greenwood G, Hashmi MZ, Liu XD *et al.* 2015. Elevation-dependent warming in mountain regions of the world. *Nature Climate Change* 5: 424.

Perez TM, Stroud JT, Feeley KJ. 2016. Thermal trouble in the tropics. *Science* 351: 1392–1393.

Pinheiro J, Bates D, DebRoy S, Sarkar D, R Core Team. 2021. *nlme: linear and nonlinear.* [WWW document] URL https://CRAN.R-project.org/package=nlme [accessed 30 March 2023].

R Core Team. 2022. *R: a language and environment for statistical computing.* Vienna, Austria: R Foundation for Statistical Computing. [WWW document] URL https://www.R-project.org [accessed 30 March 2023].

Raven JA. 2013. Rubisco: still the most abundant protein of Earth? *New Phytologist* 198: 1–3.

Rehm EM, Feeley KJ. 2015. The inability of tropical cloud forest species to invade grasslands above treeline during climate change: potential explanations and consequences. *Ecography* 38: 1167–1175.

Reich PB, Sendall KM, Stefanski A, Wei X, Rich RL, Montgomery RA. 2016. Boreal and temperate trees show strong acclimation of respiration to warming. *Nature* 531: 633–636.

Richardson JE, Pennington RT, Pennington TD, Hollingsworth PM. 2001. Rapid diversification of a species-rich genus of neotropical rain forest trees. *Science* 293: 2242–2245.

Rowland L, Zaragoza-Castells J, Bloomfield KJ, Turnbull MH, Bonal D, Burban B, Salinas N, Cosio E, Metcalfe DJ, Ford A *et al.* 2017. Scaling leaf respiration with nitrogen and phosphorus in tropical forests across two continents. *New Phytologist* 214: 1064–1077.

Ruiz-Carrascal DR, Maya MDPA, Lagoueyte MEG, Jaramillo PAZ. 2012. Aumento del Estrés Climático en los Ecosistemas Altoandinos de la Cordillera Central de Colombia. *Cambio Climático y Biodiversidad en los Andes Tropicales* 209–219.

Rustad L, Campbell J, Marion G, Norby R, Mitchell M, Hartley A, Cornelissen J, Gurevitch J. 2001. A meta-analysis of the response of soil respiration, net nitrogen mineralization, and aboveground plant growth to experimental ecosystem warming. *Oecologia* 126: 543–562.

dos Santos Pereira HA, da Costa GS, Schilling AC, Mielke MS, Sanches MC, Dalmolin ÂC. 2019. Photosynthesis, growth, and biomass allocation responses of two *Inga* species to contrasting light. *Acta Physiologiae Plantarum* 41: 1–9.

Scafaro AP, Xiang S, Long BM, Bahar NH, Weerasinghe LK, Creek D, Evans JR, Reich PB, Atkin OK. 2017. Strong thermal acclimation of photosynthesis in tropical and temperate wet-forest tree species: the importance of altered Rubisco content. *Global Change Biology* 23: 2783–2800.

Scatena FN, Bruijnzeel LA, Bubb P, Das S. 2010. Setting the stage. In: Bruijnzeel LA, Scatena FN, Hamilton LS, eds. *Tropical montane cloud forests: science for conservation and management.* Cambridge, UK: Cambridge University Press, 3–13.

Schneider CA, Rasband WS, Eliceiri KW. 2012. NIH image to IMAGEJ: 25 years of image analysis. *Nature Methods* 9: 671–675.

Sendall KM, Reich PB, Zhao C, Jihua H, Wei X, Stefanski A, Rice K, Rich RL, Montgomery RA. 2015. Acclimation of photosynthetic temperature optima of temperate and boreal tree species in response to experimental forest warming. *Global Change Biology* 21: 1342–1357.

Slot M, Kitajima K. 2015. General patterns of acclimation of leaf respiration to elevated temperatures across biomes and plant types. *Oecologia* 177: 885–900.

Slot M, Winter K. 2017. Photosynthetic acclimation to warming in tropical forest tree seedlings. *Journal of Experimental Botany* 68: 2275–2284.

Smith NG, Keenan TF. 2020. Mechanisms underlying leaf photosynthetic acclimation to warming and elevated CO_2 as inferred from least-cost optimality theory. *Global Change Biology* 26: 5202–5216.

Smith NG, Keenan TF, Colin Prentice I, Wang H, Wright IJ, Niinemets Ü, Crous KY, Domingues TF, Guerrieri R, Yoko Ishida F *et al.* 2019. Global photosynthetic capacity is optimized to the environment. *Ecology Letters* 22: 506–517.

Spracklen DV, Righelato R. 2014. Tropical montane forests are a larger than expected global carbon store. *Biogeosciences* 11: 2741–2754.

Sullivan MJ, Lewis SL, Affum-Baffoe K, Castilho C, Costa F, Sanchez AC, Ewango C, Hubau W, Marimon B, Monteagudo-Mendoza A *et al.* 2020. Long-term thermal sensitivity of Earth's tropical forests. *Science* 368: 869–874.

Sundqvist MK, Sanders NJ, Wardle DA. 2013. Community and ecosystem responses to elevational gradients: processes, mechanisms, and insights for global change. *Annual Review of Ecology, Evolution, and Systematics* 44: 261–280.

Tarvainen L, Wittemann M, Mujawamariya M, Manishimwe A, Zibera E, Ntirugulirwa B, Ract C, Manzi OJL, Andersson MX, Spetea C *et al.* 2022. Handling the heat–photosynthetic thermal stress in tropical trees. *New Phytologist* 233: 236–250.

Tcherkez G, Boex-Fontvieille E, Mahé A, Hodges M. 2012. Respiratory carbon fluxes in leaves. *Current Opinion in Plant Biology* 15: 308–314.

Tcherkez G, Gauthier P, Buckley TN, Busch FA, Barbour MM, Bruhn D, Heskel MA, Gong XY, Crous KY, Griffin K *et al.* 2017. Leaf day respiration: low CO_2 flux but high significance for metabolism and carbon balance. *New Phytologist* 216: 986–1001.

Tito R, Vasconcelos HL, Feeley KJ. 2020. Mountain ecosystems as natural laboratories for climate change experiments. *Frontiers in Forests and Global Change* 3: 38.

Tjoelker MG, Oleksyn J, Reich PB. 2001. Modelling respiration of vegetation: evidence for a general temperature-dependent Q_{10}. *Global Change Biology* 7: 223–230.

Vårhammar A, Wallin G, McLean CM, Dusenge ME, Medlyn BE, Hasper TB, Nsabimana D, Uddling J. 2015. Photosynthetic temperature responses of tree species in Rwanda: evidence of pronounced negative effects of high temperature in montane rainforest climax species. *New Phytologist* 206: 1000–1012.

Wang H, Atkin OK, Keenan TF, Smith NG, Wright IJ, Bloomfield KJ, Kattge J, Reich PB, Prentice IC. 2020. Acclimation of leaf respiration consistent with optimal photosynthetic capacity. *Global Change Biology* 26: 2573–2583.

Wang H, Prentice IC, Davis TW, Keenan TF, Wright IJ, Peng C. 2017. Photosynthetic responses to altitude: an explanation based on optimality principles. *New Phytologist* 213: 976–982.

Way DA, Oren R. 2010. Differential responses to changes in growth temperature between trees from different functional groups and biomes: a review and synthesis of data. *Tree Physiology* 30: 669–688.

Way DA, Yamori W. 2014. Thermal acclimation of photosynthesis: on the importance of adjusting our definitions and accounting for thermal acclimation of respiration. *Photosynthesis Research* 119: 89–100.

van de Weg MJ, Meir P, Grace J, Ramos GD. 2012. Photosynthetic parameters, dark respiration and leaf traits in the canopy of a Peruvian tropical montane cloud forest. *Oecologia* 168: 23–34.

Weerasinghe LK, Creek D, Crous KY, Xiang S, Liddell MJ, Turnbull MH, Atkin OK. 2014. Canopy position affects the relationships between leaf respiration and associated traits in a tropical rainforest in far North Queensland. *Tree Physiology* 34: 564–584.

Wittemann M, Andersson MX, Ntirugulirwa B, Tarvainen L, Wallin G, Uddling J. 2022. Temperature acclimation of net photosynthesis and its underlying component processes in four tropical tree species. *Tree Physiology.* 42: 1188–1202.

Zachos JC, Dickens GR, Zeebe RE. 2008. An early Cenozoic perspective on greenhouse warming and carbon-cycle dynamics. *Nature* 451: 279–283.

Ziegler C, Dusenge ME, Nyirambangutse B, Zibera E, Wallin G, Uddling J. 2020. Contrasting dependencies of photosynthetic capacity on leaf nitrogen in early- and late-successional tropical montane tree species. *Frontiers in Plant Science* 11: 500479.

Supporting Information

Additional Supporting Information may be found online in the Supporting Information section at the end of the article.

Fig. S1 Planting strategy at each experimental site.

Fig. S2 R_{dark} measurement temperature frequency plot.

Fig. S3 Vapour pressure deficit vs g_s plots for all individual data points from A–C_i curves at each site.

Fig. S4 Scatterplots to show whether values of V_{cmax_25}, J_{max_25} and R_{dark_25} are higher at 'home' elevation or away from home (warmed or cooled) for each species in our study.

Fig. S5 Rates of V_{cmax}, J_{max} and R_{dark} on a leaf mass, N and P basis at 25°C.

Fig. S6 Rates of V_{cmax}, J_{max} and R_{dark} on a leaf mass, N and P basis at T_g.

Fig. S7 Rates of V_{cmax} for each species in our study at both 25°C and growth temperature (T_g), displayed on area, mass, N and P bases.

Fig. S8 Rates of J_{max} for each species in our study at both 25°C and growth temperature (T_g), displayed on area, mass, N and P bases.

Fig. S9 Boxplot showing A_{net} values for individual species in our study.

Fig. S10 Rates of R_{dark} for each species in our study at both 25°C and growth temperature (T_g), displayed on area, mass, N and P bases.

Fig. S11 Comparisons of rates of V_{cmax}, J_{max} and R_{dark} at 25°C and at growth temperature on a leaf area basis (μ mol m^{-2} s^{-1}) between nonfertilised and fertilised trees at each site.

Fig. S12 Relationship between V_{cmax} and R_{dark} on leaf area basis (μ mol m^{-2} s^{-1}) at 25°C and growth temperature.

Methods S1 Additional details of the process used to obtain V_{cmax} and J_{max} values from A–C_i curves.

Table S1 Tree species in this study and characteristics of their thermal distributions.

Table S2 Light intensity values set for each species when taking A–C_i measurements.

Table S3 Outputs of mixed-effects ANOVAs testing for significant differences between cold- and warm-affiliated species and between temperature treatments.

Table S4 Outputs of one-way ANOVAs testing for significant differences between values for cold-affiliated species and *I. spectabilis* at 22°C.

Table S5 Outputs of *t*-tests and ANOVAs accompanying the 'Home' vs 'Away' scatterplots.

Table S6 Results of sensitivity analyses for V_{cmax}, J_{max} and R_{dark} (25°C and T_g) at 14°C, 22°C and 26°C.

Table S7 Results of sensitivity analysis comparing V_{cmax} and J_{max} using two different sets of temperature response parameters.

Table S8 P-values of ANOVAs testing for significant differences between nonfertilised and fertilised plants for each species group, at each site.

Table S9 Sensitivity analysis of V_{cmax} and J_{max} produced using different R_{dark} values in A–C_i fitting procedure.

Please note: Wiley is not responsible for the content or functionality of any Supporting Information supplied by the authors. Any queries (other than missing material) should be directed to the *New Phytologist* Central Office.